CHAPTER 5

Physical properties of liquid crystals : Theory and experimental methods.

5.1 THEORIES OF LIQUID CRYSTALLINE PHASES :

The study of liquid crystalline behaviour provides a major challenge for contemporary theoretians. To some extent liquid crystals can be understood on the basis of the simplest of theories. The early work of Maier and Saupe[1] provided a convenient molecular field rationale for the existence of the nematic phase which depends on anisotropic dispersion forces. Landau-de Gennes theory on the other hand treats liquid crystalline behaviour as perturbation of the isotropic phase by expanding the free energy density in terms of the order parameter and its spatial derivatives[2,3]. Prior to this Onsager had predicted that a system of hard rods could exhibit a first order transition from an isotropic liquid to an orientatioally ordered phase without the need for attractive forces[4].In this case the driving force for molecular alignment is provided by the orientational entropy. Despite the success of these theories, the need still remains for a more detailed description of liquid crystalline phase behaviour.

The theories of liquid crystalline phases have been described in detail in several books[5-8]. The salient features of the mean field theories of nematic and smecticA phases in a nutshell as developed by Maier-Saupe[1] and Mc Millan[9,10] are given below.

5.1.a Maier-Saupe theory for nematic phase :

The rod like molecules of a liquid crystalline substance tend to align their long axis along a preffered direction, called the director $\hat{n}$, in a mesophase. The distribution of the molecular long axes about the director is given by an orientational distribution function $f(\cos\theta)$ asssuming cylindrical symmetry of the mesophase, where θ is the angle between the director the molecular long axes. If the molecules have no head to tail asymmetry, than $\hat{n} = -\hat{n}$, and $f(\cos\theta)$ is an even function of $\cos\theta$. The distribution function can also be written as[11]:

$$f(\cos\theta) = \sum_{L \text{ even}} \left(2L + 1 \right) / 2 \langle P_L(\cos\theta) \rangle P_L \cos\theta \qquad (5.1)$$

Where $P_L(\cos\theta)$ are the L^{th} even order Legendre polynomials, and $\langle P_L(\cos\theta) \rangle$ are the statistical average given by

$$\langle P_L(\cos\theta) \rangle = \int_0^1 P_L(\cos\theta)\, f(\cos\theta)\, d(\cos\theta) \Big/ \int_0^1 f(\cos\theta)\, d(\cos\theta) \qquad (5.2)$$

$\langle P_L \rangle$ are called the orientational order parameters of which the first member, i.e., $\langle P_2 \rangle$ is commonly called the order parameter. $\langle P_2 \rangle$ is equal to one for perfectly oriented sample and is equal to zero for randomly oriented i.e., isotropic liquid.

The angular part of the generalised mean-field potential as felt by a rigid rod like molecule can be written as,

$$V(\cos\theta) = \sum_{L \text{ even}} u_L \langle P_L \rangle P_L(\cos\theta) \qquad (5.3)$$

Where U_L are functions of distance between the central molecule and its neighbours only. Maier and Saupe assumed that the potential can be taken to be the leading term only of the sereis (5.3) i.e.,

$$V(\cos\theta) = -V \langle P_2 \rangle P_2(\cos\theta) \qquad (5.4)$$

Hence, the orientational distribution function $f(\cos\theta)$ and the partition function Z are given by

$$f(\cos\theta) = Z^{-1} \exp \left[- V (\cos\theta) / K T \right] \qquad (5.5)$$

(K being the Boltzmann constant).

$$Z = \int_0^1 \exp\left[- V(\cos\theta) \,/\, K\,T \right] d(\cos\theta) \qquad (5.6)$$

Substituting the value of $f(\cos\theta)$ as in equation (5.5) to equation (5.2), we get for L = 2

$$\langle P_2 \rangle = Z^{-1} \int_0^1 P_2(\cos\theta) \exp\left[\langle P_2 \rangle \, P_2(\cos\theta) / \, T^* \right] d(\cos\theta) \qquad (5.7)$$

Where $T^* = V/KT$

$\langle P_2 \rangle$ at different temperatures can be determined by solving this self consistent equation. For many liquid crystals the Maier-Saupe $\langle P_2 \rangle$ values agree quite well with those found experimentally.

5.1.b Mc Millan's theory for SmecticA phase.

In SmecticA phase, there is a periodic density variation along the layer normal (Z -direction) in addition to the orientational distribution of the molecular axes. Hence the normalised distribution function can be written, in this case, as,

$$f(\cos\theta, z) = \sum_{L \text{ even}} \sum_{n} A_{L,n} \, P_L(\cos\theta) \cos(2\pi n z/d) \qquad (5.8)$$

$$\text{with} \quad \int_{-1}^{1} \int_{0}^{d} f(\cos\theta, z) \, dz\, d(\cos\theta) = 1 \qquad (5.9)$$

as normalising condition, d being layer thickness.

McMillan [9,10] following Kobayashi [12,13] assumed a model potential of the following form,

$$V_m(\text{Cos}\theta,z) = -V\left[\delta\alpha\tau\ \text{Cos}(2\pi z/d) + \{\eta + \alpha\sigma\ \text{Cos}(2\pi z/d)\}\ P_2(\text{Cos}\theta)\right] \tag{5.10}$$

Where α and δ are constants which depends on the characteristics of the molecules.

$\eta = \langle P_2(\text{Cos}\theta)\rangle$, $\tau = \langle \text{Cos}\theta(2\pi z/d)\rangle$ and $\sigma = \langle P_2(\text{cos}\theta)\text{Cos}(2\pi z/d)\rangle$ are the orientational, transitional and mixed order parameters respectively, and $\langle\ \rangle$ denotes statistical average of the quantities inside.

The distribution function can be written as

$$f_M(\text{Cos}\theta,z) = Z^{-1} \exp\left[-V_M\ (\text{Cos}\theta,z)\ /\ KT\right] \tag{5.11}$$

where the partition function

$$Z = \int_0^1 \int_0^d \exp\left[-V_M\ (\text{Cos}\theta,z)/\ KT\right] d(\text{Cos}\theta)\ dz \tag{5.12}$$

Once again, three self consistency equation containing η, τ and σ can be written and solved iteratively.

Out of several solutions, the equilibrium state is identified by the minimum value of free energy.

In general, we get the following three cases :

Case I : $\eta = 0$, $\tau = 0$, $\delta = 0$, isotropic liquid.

Case II : $\eta \neq 0$, $\tau = 0$, $\delta = 0$, nematic liquid crystal

Case III : $\eta \neq 0$, $\tau \neq 0$, $\delta \neq 0$, smectic liquid crystal.

5.2 Experimetal Observation :

5.2a Texture Studies :

The texture are the complex optical patterns of liquid crystalline samples observed microscopically, usually in polarised light. These are nothing but the defects of the phase structure

which are generated by the combined action of the phase structure and the surrounding glass plates. Change in texture at particular temperature indicates the occurance of phase transition. For the determination of transition temperatures and the identification of different mesomorphic phases, observation of textures is an important tool for the scientists dealing with liquid crystals. Again for a given structure, different textures can exist, depending on the spacial conditions in preparation of the sample.

It is seen that, homeotropic textures are observed only in phases of nematic, smecticA and smecticB (both orthogonal smectic phases). In smecticC, smecticF and smecticI phases (all tilted smectic phases) broken focal conic texture are observed. The inlayer ordered smectic phases show mosaic texture. Classification of different liquid crystalline phases by the texture study alone is often ambiguous, and therefore other methods are needed to support it.

5.2b X-ray diffaction from mesophases :

X-ray diffraction from mesomorphic phases has been reviewed by many workers[14-20], specially by Vainshtein and Leadbetter.

The x-ray diffraction patterns of the nematic and smectic mesophase are shown in figure 5.1 (a) & (b). In the nematic phase, the diffraction pattern consists of two different rings. The inner ring at small Bragg angle, appears along $\hat{n}$, and outer ring corresponding to the average intermolecular distance D appears along the direction perpendicular to $\hat{n}$. The diffuse rings of unoriented nematic change into cresent-shaped spots in aligned samples as shown in figure 5.1. In the smectic phases, the diffuse inner x-ray diffraction spot changes into a sharp reflection, demonstrating that these phases posses one dimensional transitional order. However, the diffraction peaks are not infinitely sharp delta function characteristics of true crystalline structure.

The angular distribution of the x-ray intensity around the outer

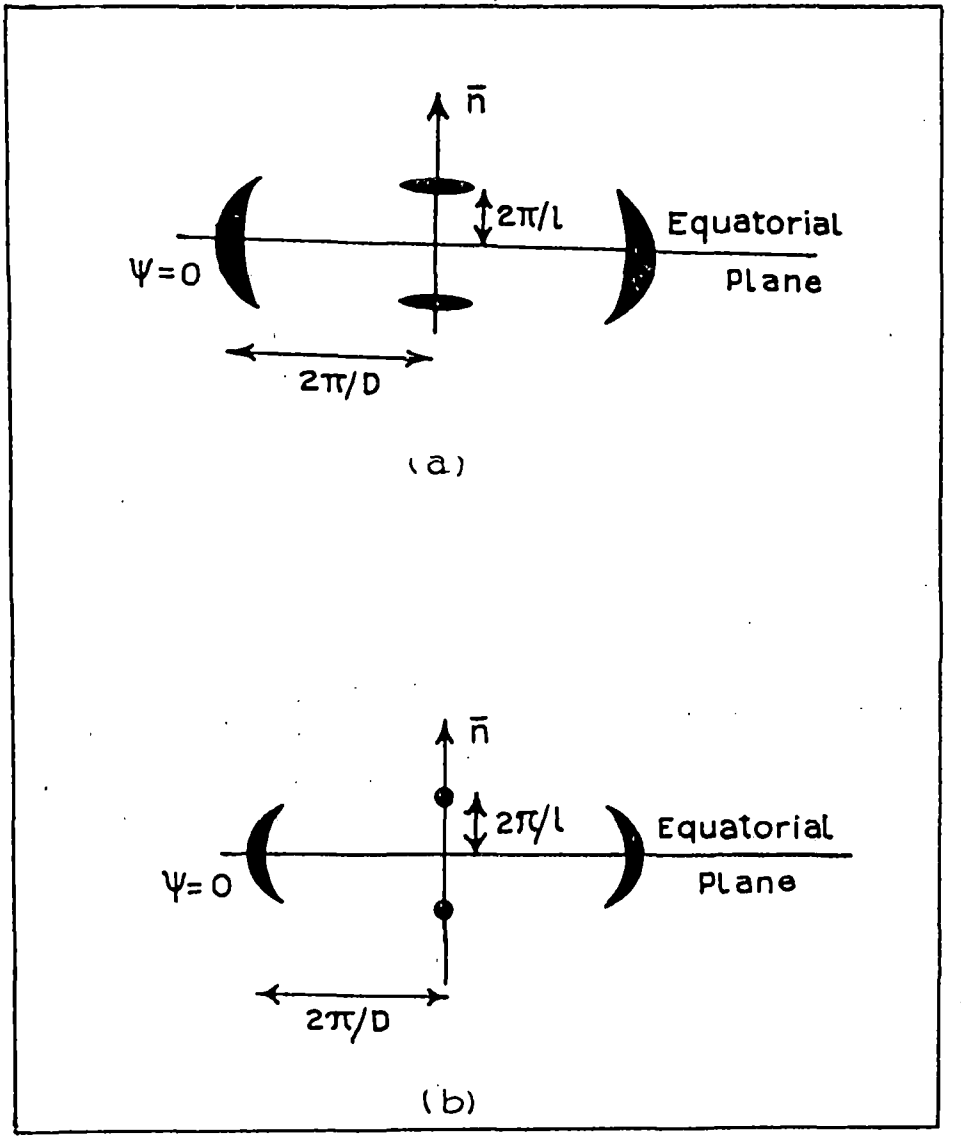

Figure 5.1 : Schematic representation of x-ray diffraction patterns of the (a) Nematic and (b) Smectic A phase.

halo (figure 5.1) also gives the orientational distribution function $f(\mathrm{Cos}\beta)$ and order parameters $\langle P_2 \rangle$.

Orientational Distribution Functions and Order Parameters :

For a system of cylindrically symmetric molecules one can define an orientational distribution function $f(\beta)$, which gives an average state of orientation of the long axis of the molecules relative to the director[14]. From the x-ray diffraction photographs we get intensities averaged over a relatively long time and over a macroscopic volume so that it can be assumed that the molecules have an averaged cylindrical symmetry even if they do not rotate about their long axis[15]. The order parameters $\langle P_L \rangle$ for a system of rigid rods in a uniaxial phase as defined in section 5.1a can be written as,

$$\langle P_L \rangle = \frac{\int_0^{\pi/2} P_L(\mathrm{Cos}\beta)\, f(\beta)\, \mathrm{Sin}\beta\, d\beta}{\int_0^{\pi/2} f(\beta)\, \mathrm{Sin}\beta\, d\beta} \qquad (5.13)$$

Where $P_L(\mathrm{Cos}\beta)$ is well known Legendre polynomial of order L. Putting L = 2 and L = 4 we get $\langle P_2 \rangle$ and $\langle P_4 \rangle$ from equation (5.13). In relating the x-ray intensities $I(\psi)$ around the diffuse equatorial arc (Fig. 5.1) with the orientational distribution function, Leadbetter and Norries[15] assumed the molecules as rigid rods perfectly aligned in clusters of a small number of molecules and obtained

$$I(\psi) = C \int_{\beta=\psi}^{\pi/2} f_d(\beta)\, \sec^2\psi \left[\tan^2\beta - \tan^2\psi \right]^{-1/2} \mathrm{Sin}\beta\, d\beta \qquad (5.14)$$

where $f_d(\beta)$ describes the distribution function of the clusters in which the molecules are perfectly aligned. Moreover, they assumed that for a perfectly aligned sample $\left[f_d(\beta)=\delta(\beta)\right]$, the scattering is zero except for the directions of the scattering vector perpendicular to the cluster axis. They have calculated the effects showning that the deviations are negligible except for highly ordered phases ($\langle P_2 \rangle \geq 0.8$). Comparing the values of $f_d(\beta)$ with $f(\beta)$ of the same sample obtained by other methods it has been seen that $f_d(\beta)$ can be replaced by $f(\beta)$ values, the true distribution function. Because of centro-symmetric molecular distribution in nematic phase, the orientational distribution function can be expanded in the form

$$I(\psi) = \sum_{n=0}^{r} a_{2n} \, \mathrm{Cos}^{2n}\psi \qquad (5.15)$$

$$f(\beta) = \sum_{n=0}^{r} b_{2n} \, \mathrm{Cos}^{2n}\beta \qquad (5.16)$$

Substituting $\mathrm{Sin}\alpha = \mathrm{Cos}\beta \, \mathrm{Sec}\psi$ in equation (5.14) we get

$$I(\psi) = C \int_0^{\pi/2} f_1(\alpha) \, \mathrm{Sin}\alpha \, d\alpha \qquad (5.17)$$

From equations (5.15), (5.16) and (5.17) we have

$$\sum a_{2n} \, \mathrm{Cos}^{2n}\psi = \int_0^{\pi/2} \sum_{n=0}^{r} b_{2n} \, \mathrm{Cos}^{2n}\psi \, \mathrm{Sin}^{2n+1}\alpha \, d\alpha$$

$$= \sum_{n=0}^{r} b_{2n} \, \mathrm{Cos}^{2n}\psi \int_0^{\pi/2} \mathrm{Sin}^{2n+1}\alpha \, d\alpha \qquad (5.18)$$

Since ψ is arbitrary, the coefficient of $\mathrm{Cos}^{2n}\psi$ must be equal. Now,

$$\int_0^{\pi/2} \mathrm{Sin}^{2n+1}\alpha \, d\alpha = \frac{2^{2n}\,(n\,!)^2}{(2n+1)\,!}$$

and so

$$b_{2n} = a_{2n} \frac{(2n+1)\,!}{2^{2n}\,(n!)^2} \qquad (5.19)$$

The series in equations (5.15) and (5.16) converge rapidly. Retaining eight terms in the truncated series, a least square fitting was made to obtain the coefficients from equations(5.15) with corrected intensity values. The calculated intensity values in all cases were found to be in good agreement with the observed intensities. This values of a_{2n} were then used to calculate the coefficients of b_{2n}. Then, $f(\beta)$ values were calculated using eight terms in the series in equation (5.16).

By calculating the integral,

$$\int_0^{\pi/2} f(\beta)\, \mathrm{Sin}\beta \, d\beta = A \quad \text{(say)},$$

and then dividing all the b_{2n} values by A we obtained the normalised values of the orientational distribution function.

Substituting equation (5.16) in equation (5.13) we get

$$\langle P_2 \rangle = 1/2 \; \frac{\int_0^1 \left(3\,\mathrm{Cos}^2\beta - 1 \right) \sum_{n=0}^{r} b_{2n}\, \mathrm{Cos}^{2n}\beta \, d(\mathrm{Cos}\beta)}{\int_0^1 \sum_{n=0}^{r} b_{2n}\, \mathrm{Cos}^{2n}\beta \, d(\mathrm{Cos}\beta)} \qquad (5.20)$$

This can be written in the form of standard integrals and $\langle P_2 \rangle$

can be calculated. Similarly, $\langle P_4 \rangle$ can also be calculated. Vainshtein obtained a fairly good approximation for the order parameter by replacing $f(\beta)$ values with $I(\psi)$ values at a certain Bragg angle in equation (5.13).

Molecular parameters for x-ray studies :

The average lateral distance between the neighbouring molecules (D) was calculated from the x-ray diffraction photographs by a formula given by[21]

$$2D \sin\theta = K\lambda \qquad (5.21)$$

K is a constant which comes from the cylindrical symmetry of the system. Recent calculations[22] have shown that the value of K depends on the order parameter of the sample under consideration. For perfectly ordered state K = 1.117 as given by de Vries[23]. However, since the variation of K with $\langle P_2 \rangle$ is small, we have used the value K = 1.117 for all our calculations.

For both oriented and unoriented samples the Bragg equation was used ($2d\sin\theta = \lambda$) to calculate the apparent molecular length or layer thickness, where θ is the Bragg angle for inner diffraction maxima.

Experimental technique and data analysis :

X-ray diffraction photographs were obtained with the apparatus described below using nickel filtered CuKα radiation in the transimission geometry on a film, using a flat plate camera designed in our laboratory by Jha et al[24].(Figure 5.2). X-ray diffraction photographs were taken at different temperatures in the presence of a magnetic field. The sample was taken in thin walled lithium glass capillary of 1mm diameter. The capillary containing sample was placed in a brass block. The temperature of the block was controlled within $\pm 0.5^{\circ}C$ by a temperature controller (Indotherm MD 401). The sample was first heated to the isotropic phase and magnetic field

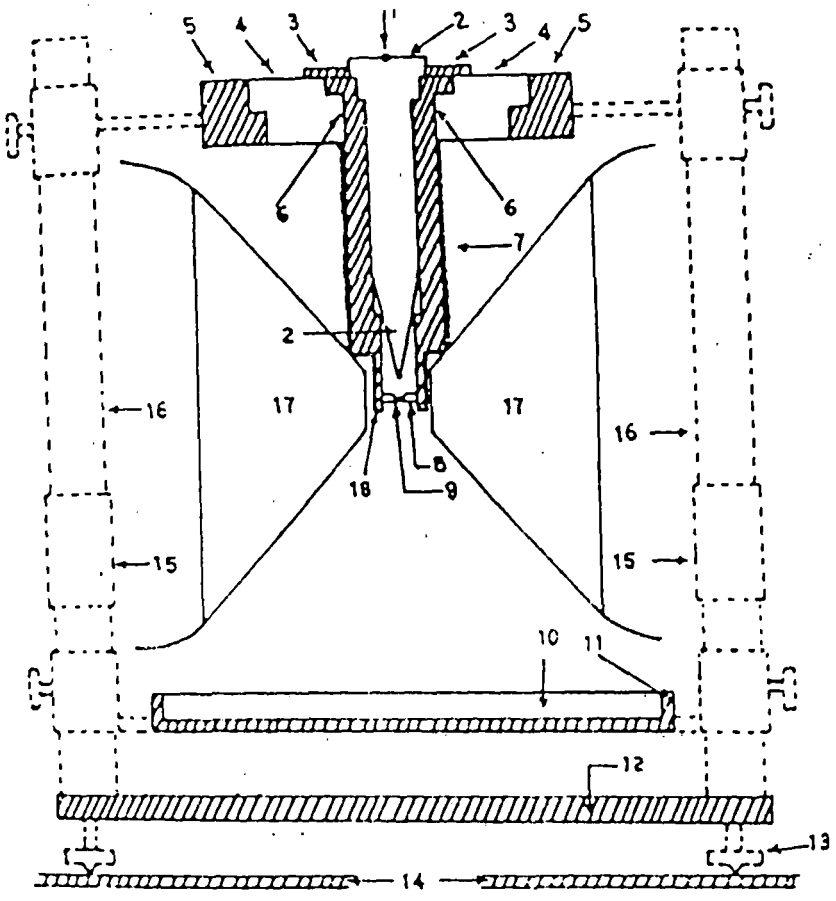

Figure 5.2 : Sectional diagram of the x-ray diffraction camera. 1 - X-ray, 2 - Collimator, 3 - Brass ring, 4 - Ring of sindanyo board, 5 - Brass ring, 6 - Cylindrical brass chamber, 7 - Asbestos insulation and heater winding, 8 - Specimen holder and thermocouple, 9 - Sample, 10 - Film cassette, 11 - Film cassette holder, 12 - Base plate, 13 - Levelling screw, 14 - Brass plates over the coils of the electromagnet, 15 - Removable spacer, 16 - Supporting brass stand, 17 - Pole pieces, 18 - Asbestos insulation.

was applied parallel to the capillary axis. The substance was allowed to cool to the desired temperature in presence of the magnetic field. The strength of the magnetic field was measured previously by a gaussmeter (ECIL model GH867). X-ray beam was collimated by a collimater of aperture 0.8mm. A Ni-filter of thickness 0.009mm was used to obtain predominant CuKα radiation of wavelength 1.542Å. When the temperature reached equilibrium then the x-ray tube was switched on. Photographs were taken at various constant temperatures. In case of the determination of orientational order parameters the sample to film distance was maintained at about 7cm.

For the determination of the exact distance between the sample and the film, an aluminium photograph was taken. Measuring the diameter of the diffraction rings corresponding (111) and (200) reflections and values of Bragg angles, the actual distance between sample and the film can be calculated.

(a) Conversion of optical density to x-ray intensity :

The optical density of the x-ray photographs were measured by microdensitometer (Carl Zeiss MD 100) which has a potentiometric recording (K200) facility for linear scanning. X-ray intensity values are then obtained from the conversion of the corresponding optical density values from a graph as shown in figure 5.3 .Using multiple film technique as given by Klug and Alexander[25] an intensity scale was prepared for this purpose.

(b) Circular Scaning of X-ray Photographs.

A rotating stage was fabricated in our laboratory to facilitate 360° scanning of the photographs. Photographs were scanned to measure the angular intensity distribution $I(\theta)$ which was used to calculate the orientational distribution function $f(\beta)$ and order parameters $\langle P_2 \rangle$ and $\langle P_4 \rangle$. The circular scans of the outer diffraction arc taken from $\psi = 0$ to $\psi = 360^{\circ}$ at about 1° intervals

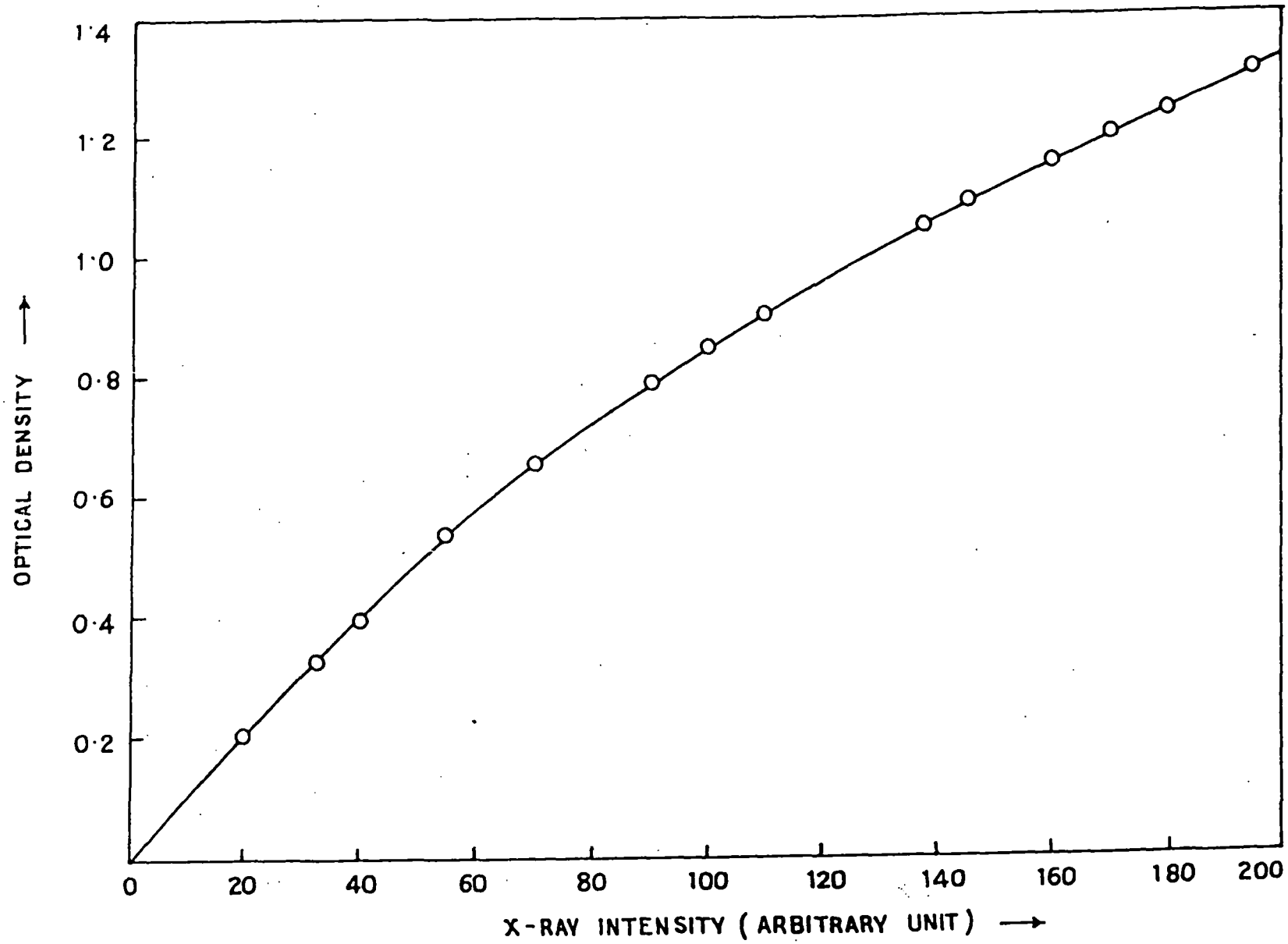

Figure 5.3 : Optical density vs. x-ray intensity curve used for calibration.

near the peak and at larger intervals elsewhere. The optical density values obtained from the densitometric circular scan where converted to x-ray intensity with the help of calibration curve. Intensity values were then corrected for background values arising due to the air scattering. The peak intensity position which corresponds to ψ = 0 was determined from angle vs intensity curve (figure 5.4). Taking nineteen $I(\psi)$ values from $\psi = 0$ to $\psi = 90^{o}$ at 5^{o} intervals from the smoothed $I(\psi)$ vs ψ curve, $f(\beta)$, $\langle P_2 \rangle$ and $\langle P_4 \rangle$ were calculated by using Leadbetter's expression. A computer program has been developed for these calculations.

(c) Linear Scaning of X-ray Photographs.

The diameter of the diffraction rings were determined from the peak positions obtained by linear scanning using a chart drive and corresponding values were calculated.

5.2c OPTICAL BIREFRINGENCE STUDY.

Theoretical considerations :

The birefringence of liquid crystals is the visible manifestation of their long-range order and it is defined only for a uniformly ordered domain. In a uniaxial liquid crystal, the ordinary refractive index n_o is perpendicular to the optic axis or director and represented as $n_\perp$ and extra-ordinary refractive index n_e is parallel to the director which is denoted as $n_\parallel$. From the measurement of n_o and n_e , we can estimate ordering in the liquid crystal at different temperatures.

In a liquid crystal the polarisation $\bar{P}$ is given by,

$$\bar{P} = N \langle \alpha . E_l \rangle \qquad (5.22)$$

where the brackets denote the average over the orientations of all molecules. $\bar{\alpha}$ is the molecular polarizability. N is the number of

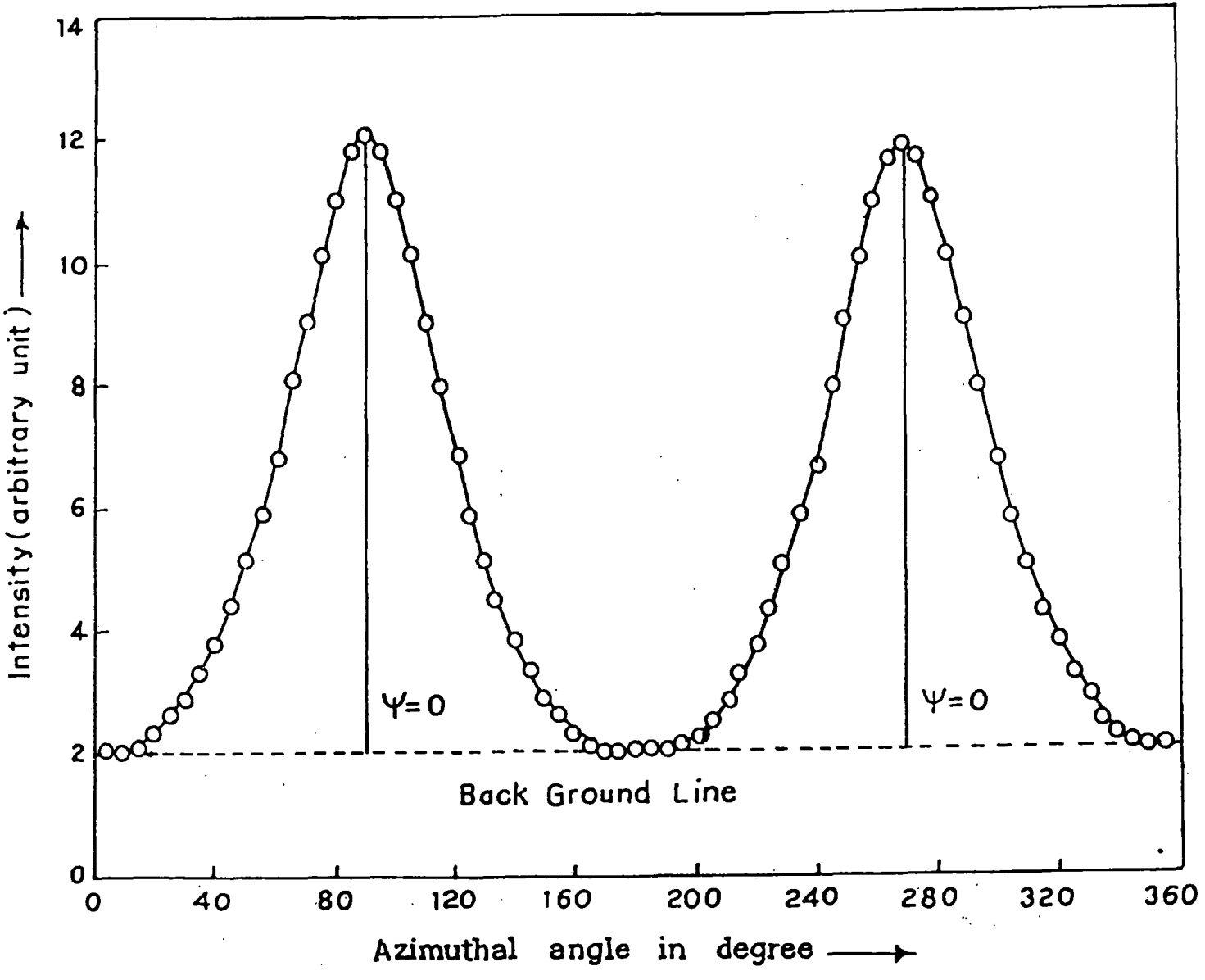

Figure 5.4 : Average intensity I(ψ) vs. azimuthal angle (ψ).

molecules per unit volume and E_i is the internal field, the average field that acts on a molecule.

The internal field is a linear function of the macroscopic field and can be represented by

$$E_i = \bar{K} \cdot E \qquad (5.23)$$

Where $\bar{K}$ is an ordinary second rank tensor. The introduction of this tensor makes it possible to write $\bar{P} = N < \bar{\alpha}.\bar{K} >E$.

Refractive index is related to polarizability by the following relation

$$n_{\parallel}^2 - n_{\perp}^2 = N \left(< \bar{\alpha}.\bar{K} >_{\parallel} - <\bar{\alpha} .\bar{K} >_{\perp} \right) \qquad (5.24)$$

So if we want to calculate molecular polarizability we must know the internal field tensor $\bar{K}$ which was ususually valid for isotropic medium.Because of anisotropy of the internal field, Lorentz-Lorentz formula can not be applied to liquid crystals. We follow, therefore, Neugebauer's relation or Vuk's formula to calculate the polarizabilities. Saupe and Maier also applied a more elaborate form of internal field suggested by Neugebauer.

(a) Neugebauer's method :

Neugabauer[26] extended Lorentz-Lorentz equations for an isotropic system to an anisotropic system. The effective polarizabilities α_e and α_o of the liquid crystals are given by

$$n_e^2 - 1 = 4\pi N \alpha_e \left(1 - N \alpha_e \gamma_e \right)^{-1} \qquad (5.25)$$

$$n_o^2 - 1 = 4\pi N \alpha_o \left(1 - N \alpha_o \gamma_o \right)^{-1} \qquad (5.26)$$

Where N is the number of molecules per cc and γ_i's are internal field constants, n_e and n_o the extra-ordinary and ordinary refractive indices respectively. The equations for calculating the

α_o and α_e obtained from equations (5.25) and (5.26) are

$$\frac{1}{\alpha_e} + \frac{2}{\alpha_o} = \frac{4\pi N}{3}\left[\frac{n_e^2 + 2}{n_e^2 - 1}\right] + \left[\frac{2(n_o^2 + 2)}{n_o^2 - 1}\right] \qquad (5.27)$$

and $$\alpha_e + 2\alpha_o = \frac{9}{4\pi N}\left[\frac{n^2 - 1}{n^2 + 2}\right] \qquad (5.28)$$

where, $n^2 = 1/3\ (n_e^2 + 2n_o^2)$

Solving equations (5.27) and (5.28) α_o and α_e can be obtained.

(b) Vuk's method.

Vuks[27] has derived another formula for polarizabilities associated with anisotropic organic molecules. The principal polarizabilities and refractive indices can be expressed as,

$$\frac{n_i^2 - 1}{n^2 + 2} = \frac{4\pi N}{3}\alpha_i , \quad i = x,y,z \qquad (5.29)$$

where $n^2 = 1/3 \sum_i n_i^2$

So we find, $$\frac{n_o^2 - 1}{n^2 + 2} = \frac{4\pi N}{3}\alpha_o \qquad (5.30)$$

$$\frac{n_e^2 - 1}{n^2 + 2} = \frac{4\pi N}{3}\alpha_e \qquad (5.31)$$

where $n^2 = 1/3\ (2n_o^2 + n_e^2)$; n being mean refractive index. α_e and α_o can be calculated directly from the refractive index values.

Additive Rule of Bond Polarizability.

Denbigh - Le Fevre[28] established a simple sum rules for the

calculation of molecular polarizability in terms of mean bond polarizability. Molecular polarizabilities for all the substances have been calculated from this additive rule and compared with the values obtained from Vuk's and Neugebauer's methods.

Calculation of order parameters from polarizabilities :

The principal polarisabilities (α_o,α_e) have been calculated by using Vuk's (isotropic model)and Neugabauer's relations (anisotropic model). It can be shown that

$$\alpha_e = \bar{\alpha} + 2/3\ \alpha_a \langle P_2 \rangle \qquad (5.32)$$

$$\alpha_o = \bar{\alpha} - 1/3\ \alpha_a \langle P_2 \rangle \qquad (5.33)$$

Where $\bar{\alpha} = (2\alpha_o + \alpha_e)/3$ is the mean polarizability. $\alpha_a = (\alpha_{\parallel} - \alpha_{\perp})$ is the molecular polarizability anisotropy where $\alpha_{\parallel}$ and $\alpha_{\perp}$ are the principal polarizabilities, parallel and perpendicular to the long axes of the molecules in the crystalline state.

To get the values of $(\alpha_{\parallel} - \alpha_{\perp})$, when solid phase data is not available, the widely used method of Haller[29] et. al was adopted. A graph was plotted with $\log(\alpha_e - \alpha_o)$ vs $\log.(T_c - T)$, where T_c corresponded to the nematic isotropic transition temperature. The plot which is found to be a straight line is extrapolated to $T=0$, giving $(\alpha_e - \alpha_o)_{T=0} = (\alpha_{\parallel} - \alpha_{\perp})$. For each case a set of values of α_e, α_o and $(\alpha_{\parallel} - \alpha_{\perp})$ were obtained (figure 5.5) and then from the relation

$$\langle P_2 \rangle = \frac{\alpha_e - \alpha_o}{\alpha_{\parallel} - \alpha_{\perp}} \qquad (5.34)$$

Order parameter $\langle P_2 \rangle$ was calculated.

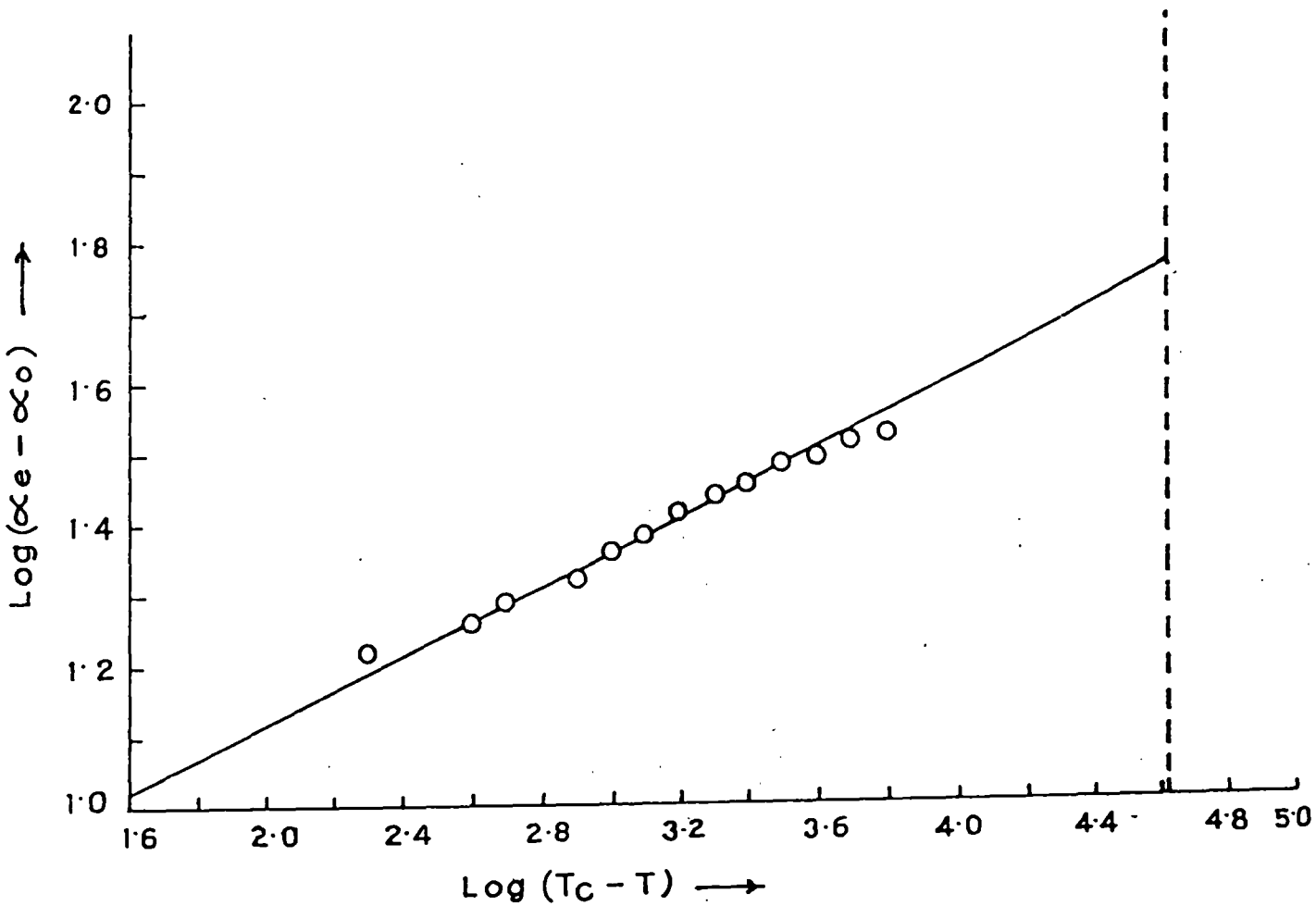

Figure 5.5 : Typical $\log(\alpha_e - \alpha_o)$ vs. $\log(T_c - T)$ curve
(Sample - 1d(1)CC, Chapter - 6).

Measurement of refractive indices :

The refractive indices n_e and n_o fo extra-ordinary and ordinary ray were measured by a thin prims technique. The refracting angle of the prism was less than 2^o. The details of the preparation of the prism and the experimental procedure have already been reported by Zeminder et al[30]. For the preparation of a prism two clean optically plane glass plates were used. One surface of each of the glass plates was rubbed parallel to the direction of one of their edges. The plates were then treated with a dilute solution of polyvinyl alcohol and then dried. The prefered direction on the substrate can be obtained by rubbing the same surface in the same direction again by a tissue paper. The prism was then formed by placing the treated surfaces inside and the rubbing direction parallel to the refracting edge of the prism. The sides of the prism were sealed with a high temperature adhesive. Now the liquid crystal sample was allowed to flow inside the prism by melting a few crystals at the top. The sample was heated to the isotropic state and then cooled down very slowly to the desired temperature. This process was repeated several times. No magnatic field was applied. Repeated heating and cooling produced a homogeneous namatic sample with optic axis parallel to the refracting edge of the prism. The prism was then placed in a brass chamber, whose temperature could be maintained by a temperature controller (Indotherm model 401) at any desired value to an accuracy of $\pm$ 0.5^{o}C by means of an electric heater. The refractive indices were measured for three wave-lengths (λ = 6907Å , 5890Å , 5461Å) from a murcury lamp by means of a precision spectrometer, a wavelength selector and a Nicol prism.

5.2d Measurement of Densities :

The densities of the liquid crystals were measured with the help a dilatometer of the capillary type. A weighed sample of the liquid crystal was introduced inside the capillary tube of the

dilatometer and it was placed in a thermostated water bath. Sufficient time was allowed for equilibrium at the desired temperature before taking each reading. The length of the liquid crystal column was measured at different temperatures with a travelling microscope. The densities were calculated after correction for the expansion of the glass. The accuracy of the measurement of the densities were within 0.1%.

5.2e. THEORETICAL CALCULATION OF ELECTRIC DIPOLE MOMENT.

Guggenheim[31] showed a simpler way of calculating electric dipole moment of a polar solute dissolved in a non-polar solvent at a temperature T. Provided the solution is suffficiently dilute for mutual interaction between solute molecules to be negligible, partial molar volume V_1 of solvent and partial molar volume V_2 of solute are constants. According to Debye the basic formulae for the determination of electric dipole moment μ from the measurements of ε and n are

$$\frac{\varepsilon - 1}{\varepsilon + 2}\,\bar{V} = \frac{\varepsilon_o - 1}{\varepsilon_o + 2} V_1(1 - x) + \frac{4\pi N}{3}\left(\gamma_e + \gamma_a + \frac{\mu^2}{3KT}\right) x \qquad (5.35)$$

$$\frac{n^2 - 1}{n^2 + 2}\,\bar{V} = \frac{n_o^2 - 1}{n_o^2 + 2} V_1(1 - x) + \frac{4\pi N}{3}\gamma_e x \qquad (5.36)$$

The notations used in the above equations are,

x = Mole fraction of solute.

C = Concentration of solute expressed as moles/volume

$\bar{V}$ = Mean molar volume.

ε = Dielectric constant of solution.

ε_o = Dielectric constant of pure solvent.

n = Refractive index of solution.

n_o = Refractive index of pure solvent.

γ_e = Electronic contribution to polarizability of solute molecule

γ_a = Atomic contribution to polarizability of solute molecule.

K = Boltzmann's constant

N = Avogadro's number.

V_1 and V_2 are related with $\bar{V}$ as

$\bar{V} = (1 - x)V_1 + x V_2$ and $C = x/V$

From equation (1) and (2) we can write,

$$\left[\frac{\varepsilon - 1}{\varepsilon + 2} - \frac{n^2 - 1}{n^2 + 2}\right]\bar{V} = \left[\frac{\varepsilon_o - 1}{\varepsilon_o + 2} - \frac{n_o^2 - 1}{n_o^2 + 2}\right]V_1(1 - x) + \frac{4\pi N}{3}\left[\gamma_a + \frac{\mu^2}{3KT}\right]x \qquad (5.37)$$

For no atomic contribution to the polarizability of either solvent or solute molecules , we can write $\varepsilon_o = n_o^2$ and $\gamma_a = 0$ and equation (5.37) can be written as,

$$\left[\frac{\varepsilon - 1}{\varepsilon + 2} - \frac{n^2 - 1}{n^2 + 2}\right] = \frac{4\pi N}{3}\frac{\mu^2}{3KT}C \qquad (5.38)$$

According to equation (5.38) if the experimental quantity,

$$\left[\frac{\varepsilon - 1}{\varepsilon + 2} - \frac{n^2 - 1}{n^2 + 2}\right] = \frac{3(\varepsilon - n^2)}{(\varepsilon+2)(n^2+2)} \qquad (5.39)$$

were plotted against C , then a straight line is obtained through the origin having a slope equal to $4\pi N\mu^2/9KT$.

But due to the atomic polarizability of the solvent, $\varepsilon_o = n_o^2$. Guggenheim then defined a fictitious atomic polarizability γ'_a expressed by the equation,

$$\frac{4\pi N}{3}\gamma'_a = \left[\frac{\varepsilon_o - 1}{\varepsilon_o + 2} - \frac{n_o^2 - 1}{n_o^2 + 2}\right]\frac{V_2}{V_1} \qquad (5.40)$$

Now from equations (5.37) and (5.40) we obtain ,

$$\left[\frac{\varepsilon - 1}{\varepsilon + 2} - \frac{n^2 - 1}{n^2 + 2}\right] = \left[\frac{\varepsilon_o - 1}{\varepsilon_o + 2} - \frac{n_o^2 - 1}{n_o^2 + 2}\right] + \frac{4\pi N}{3}\left[\gamma_a - \gamma'_a + \frac{\mu^2}{3KT}\right]C \qquad (5.41)$$

According to equation (5.41), if the experimental quantity $3(\varepsilon-n^2)/(\varepsilon+2)(n^2+2)$ is plotted against C , the curve has an

initial height $\left[\frac{\varepsilon_o - 1}{\varepsilon_o + 2} - \frac{n_o^2-1}{n_o^2+2}\right] = \frac{3(\varepsilon_o - n_o^2)}{(\varepsilon_o+2)(n_o^2+2)}$ (5.42)

and an initial slope $\frac{4\pi N}{3}\left[\gamma_a - \gamma'_a + \frac{\mu^2}{3KT}\right]$.

Since it is only the initial slope that is of interest so it was further simplified by equating the denominator of equations (5.39) and (5.42) we then have

$$3(\varepsilon - n^2) = 3(\varepsilon_o - n_o^2) + \frac{4\pi N}{3}(\varepsilon_o+2)(n_o^2+2)\left[\gamma_a - \gamma'_a - \frac{\mu^2}{3KT}\right]C$$

$$\text{or, } (\varepsilon - n^2) - (\varepsilon_o - n_o^2) = \frac{4\pi N}{9}(\varepsilon_o+2)(n_o^2+2)\left[\gamma_a - \gamma'_a - \frac{\mu^2}{3KT}\right]C \qquad (5.43)$$

Thus plotting the experimental quantity $(\varepsilon-n^2)$ against C , a curve is obtained having an initial height $(\varepsilon_o-n_o^2)$ and an

initial slope,

$$\frac{(\varepsilon_o+2)(n_o^2+2)}{3}\,\frac{4\pi N}{3}\left[\gamma_a-\gamma'_a-\frac{\mu^2}{3KT}\right]$$

For polar solute molecules , at least those having μ greater than one debye, γ_e is itself usually small compared with $\mu^2/3KT$. It is found that γ_a is always less than one-tenth of γ_e. Hence an accurate estimate of γ_a is not needed. Under these circumstances, the simplest assumption can be made as $\gamma_a = \gamma'_a$.

Thus equation (5.44) can be written as,

$$(\varepsilon - n^2) - (\varepsilon_o - n_o^2) = \frac{(\varepsilon_o + 2)\,(n_o^2 + 2)}{3} \cdot \frac{4\pi N}{3} \cdot \frac{\mu^2}{3KT}\, C$$

$$\text{or,}\quad \mu^2 = \frac{27KT\left[(\varepsilon - n^2)-(\varepsilon_o - n_o^2)\right]}{4\pi NC\,(\varepsilon_o + 2)(n_o^2 + 2)} \qquad \text{----------(5.45)}$$

This simplified equation was used for the determination of dipole moments of polar compounds which is given in detail in chapter 8.

REFERENCES :

(1) A. Saupe and W. Maier, Z. Natureforsch, 14a, 882 (1959) and 15a, 287(1960).

(2) P.G. de Gennes, Mol. Cryst. Liq. Cryst. 12, 193, (1971).

(3) P. Sheng and E. B. Priestley, P. J. Wojtowitz. eds., Introduction to Liquid Crystals, (Plenum Press) N.Y. (1974).

(4) L. Onsager, Ann. N. Y. Acad. Sci. 51, 627, (1949).

(5) S. Chandrasekhar, Liquid Crystals, Cambridge University Press, Cambridge, (1977).

(6) G. Vertogen and W. H. de Jeu, Thermotropic Liquid Crystals Fundamentals, Springer-Verlag (1988).

(7) G. R. Luckhurst and G. W. Gray, (Editors) The Molecular Physics of Liquid Crystals, Academic Press (1979).

(8) P. G. de Gennes, The Physics of Liquid Crystal, Clarendon Press, Oxford, (1974).

(9) W. L. McMillan, Phys. Rev., A4, 1238 (1971).

(10) W.L. McMillan, Phys. Rev.,A6, 936 (1972).

(11) E.B. Priestley, P.S. Pershan, R.B. Meyer and D.H. Dolphin, Vijnana Parishad Anusandhan Patrika, 14, 93 (1971).

(12) K.K. Kobayashi, J. Phys., Soc. (Japan), 29, 101 (1970).

(13) K.K. Kobayashi, Mol. Cryst. Liq. Cryst., 13, 137 (1971).

(14) B.K. Vainstein, Diffraction of X-rays by Chain Molecules, Elsevier, Pub. Co. (1966).

(15) A.J. Leadbetter, The Molecular Physics of Liquid Crystals, Eds., G. R. Luckhurst and G. W. Gray, Chapter 13, Academic Press (1979).

A.J. Leadbetter and E. K. Norris, Mol. Phys., 38, 689 (1974).

(16) I. G. Chistyakov, Sov. Phys. Vsp.9, 551 (1967).

(17) L.A. Azaroff, Mol. Cryst. Liq. Cryst., 60, 73 (1980).

(18) J. Falguerettes and P. Delord, Liquid Crystals and Plastic Crystals, Eds G.W. Gray and P.A. Winsor, Ellis Horwood, Vol. 2,

chapter 3, (1974).

(19) H. Kelker and R. Hartz, Hand book of Liquid Crystals, Verlag Chemie, Chapter 5, (1980).

(20) P.S. Pershan, Structure of Liquid Crystal Phases, World Scientific (1988).

(21) J. H. Wendroff and E. P. Price, Mol. Cryst. Liq. Cryst., 24, 129 (1973).

(22) R. Paul and G. Chaudhury, Abstract in the 14th International Liquid Crystal Conference, Pisa, (1992), Abs-no -H-P23.

(23) A. de Vries, Mol. Cryst. Liq. Cryst.,10, 31 & 219 (1970).

(24) B. Jha and R. Paul, Proc. Nucl. Phys. Solid State Phys. Symp., India, 19c, 491 (1970).

(25) H.P. Klug and L.E. Alexander, X-ray diffraction procedures, John Willey and Sons, N.Y. Page 114 & 473 (1974).

(26) H.E. Neugebauer, Canad. J. Phys., 32, 1 (1954).

(27) M.F. Vuks, Optics and Spectroscopy, 20, 361 (1966).

(28) R. J. W. Le Fevre, Adv. Org. Chem., 3, 1 (1965).

(29) I. Haller, H. A. Huggins, H. R. Lilienthal and T. R. McGuire, J. Phys. Chem., 77, 950 (1973).

(30) A. K. Zeminder, S. Paul and R. Paul, Mol. Cryst. Liq. Cryst., 61, 191 (1980).

(31) E. A. Guggenheim, Trans. Faraday Soc., 45, 714 (1949).